Electromagnetic interference of wireless power transfer system on wearable electrocardiogram

Electromagnetic Interference of Wireless Power Transfer System on Wearable Electrocardiogram

Wei Liao[1&2], Jingjing Shi[1], and Jianqing Wang[1,*]

[1]Graduate School of Engineering, Nagoya Institute of Technology, Japan
[2]School of Electric and Electronic Engineering, Shanghai University of Engineering Science, China
[*]wang@nitech.ac.jp

ABSTRACT

The increasing aging population is leading to a wide-scale demand for health-state monitoring by a wireless body area network (BAN). Wireless BAN needs each vital sensor to act as a wearable device for collecting blood pressure, electrocardiogram (ECG), electroencephalogram (EEG), etc. in daily life. On the other hand, wireless power transfer is also getting into our daily life because of its convenience, which suggests a potential electromagnetic interference (EMI) problem on the wearable devices in healthcare and medical BAN. In this paper, we quantitatively evaluated the EMI on wearable ECG for 6.8 MHz wireless power transfer system. We employed electromagnetic field analysis technique to derive the common mode voltage between the human body with a wearable ECG and the ground plane, and circuit simulation or measurement to derive the interference voltage at the wearable ECG output. The result first time gave a quantitative evaluation for EMI of wireless power transfer on wearable ECG. The approach is also available to be applied to EMI evaluation of other wearable devices in healthcare or medical applications.

Introduction

The increasing aging population is leading to a wide-scale demand for health-state monitoring in daily life. Wireless body area network (BAN) provides an effective means to collect various vital data and send them wirelessly to a hospital or medical center. In wireless BAN, a vital sensor usually is a wearable device with wireless communication function. It can automatically collect the vital data such as blood pressure, electrocardiogram (ECG), or electroencephalogram (EEG) in daily life, and forward the data to medical staffs in a hospital or medical center in a real time for healthcare administration or medical applications [1]-[4]. For example, in [5] we developed a new wearable ECG based on human body communication (HBC) technology. As shown in Fig. 1, the wearable ECG consists of a pair of sensing electrodes, a detection circuit, and a wireless transceiver. It is attached on the chest, acquires the ECG data continuously, and sends out them to a personal computer in a real time. The ECG data collected in the personal computer can be used for various healthcare or medical applications.

On the other hand, wireless power transfer is also getting into our daily life due to its convenience. Efficient wireless power transfer has been achieved by electromagnetic resonance, and is being used in wireless charging cellular phones or electric cars [6][7]. Resonant wireless power transfer systems typically operate in the low MHz range, which may be a potential of electromagnetic interference (EMI) with a wearable device such as wearable ECG. So far, the EMI problem for wearable healthcare devices is mainly focused on commercial power frequency bands. In fact, the electromagnetic field produced by wireless power transfer can couple into the wearable ECG through the sensing electrodes to cause an interference voltage in the detected ECG signals. But to our knowledge, there is no study about how to quantify such interference from a wireless power transfer system.

In this study, we employ a two-step approach [8] to evaluate the EMI level at the wearable ECG for a typical 6.8 MHz wireless power transfer system. In the first step, we derive the EMI voltages produced between the ECG sensing electrode and ground plane as a common mode voltage by EM field simulation/measurement, while in the second step, we derive the interference voltage in the ECG signals by an electric circuit analysis or simulation/measurement. Such an approach provides an effective means to quantitatively evaluate the EMI for a wearable device in the design stage or actual use.

Analysis Model and Method

Fig. 2 shows the numerical model of a 6.8 MHz wireless power transfer system with a human body [9][10] for EMI evaluation. The human body is irradiated by the single-sided (transmitter only) wireless power transfer system operating at 6.8 MHz. The transmitter is comprised of a drive loop and a high-Q transmit coil, and the receiver has the same structure. The drive loop is a single-turn loop with an outer diameter of 305 mm. The transmit coil is a spiral with 6.1 turns, an outer diameter of 580 mm

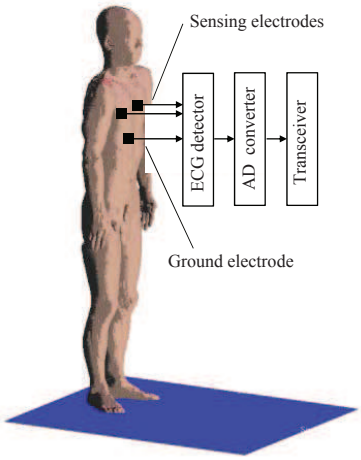

Figure 1. Wearable ECG on human body.

and a pitch of 10 mm. The loop to coil distance is 135 mm. The diameter of the copper wire is 2.54 mm for both the coil and loop. In the EMI evaluation, the drive loop and transmit coil are set with either horizontal or vertical arrangement, and the nearest distance is d between the transmit coil and the human body.

The human stands on a ground plane, and wears a wearable ECG on the chest. The wearable ECG has two sensing electrodes and one ground electrode. All of them have a square plate structure. The two sensing electrodes are attached to the chest directly or through a capacitive coupling, respectively, for ECG signal acquisition. The ECG signals acquired from the two sensing electrodes are then filtered and differentially amplified with an operational amplifier (opamp). The low pass filter (LPF) and high pass filter (HPF) are used respectively to remove the direct-current (DC) component, drift noises, and high frequency interference noises. They have a cutoff frequency of around 100 Hz for the LPF and 10 Hz for the HPF, respectively, and an attenuation of around 30 dB outside the pass bands. A notch filter is also used to cut the commercial power frequency of 50/60 Hz. The circuit amplifies differentially the signals from the two sensing electrodes and adjusts their levels to fall into the analog input range of an analog-to-digital converter (ADC). The AD-converted ECG signals are transmitted by a wireless technology such as Bluetooth or HBC transceiver. Fig. 3 shows a typical example of the ECG signal acquired by our developed HBC-based wearable ECG. As can be seen, the wearable ECG clearly acquires the Q-wave, R-wave, S-wave and T-wave with reasonable accuracy, and the ECG signal level at the detection circuit output is around 0.5 V.

Electromagnetic field from the wireless power transfer system will produce a common mode voltage between the human body and the ground plane. Since the human body is approximately a conductor at the considered frequency, the potentials on the human body for both the sensing electrode and the ground electrode attachment locations have the almost same value. By integrating the produced electric field along a route from the ground plane to the human body, we can obtain a voltage between the human body and the ground plane, which is known as the common mode voltage. The common mode voltage cannot be rejected in the differential stage of the ECG detection circuit if there is an impedance imbalance between these electrodes, and will be coupled into the ECG detection circuit through the sensing electrodes and ground electrode.

Fig. 4 shows the common-mode equivalent circuit of the wearable ECG. The interference voltage V_c is between the human body and the ground plane, here we denotes which as the earth ground. When the two sensing electrodes touch the human body directly, there will be a contact resistance R_{ea} or R_{eb} between the human body and the input of detection circuit. While when the two sensing electrodes do not touch the human body directly, there will be a coupling capacitance C_{ea} or C_{eb} between the human body and the input of detection circuit. For generality, we denote them as contact impedance Z_{ea} and Z_{eb} respectively. The two contact impedances are usually not same, i.e., are imbalanced, due to the different attachment conditions. In addition, the ground electrode has also a contact impedance between the human body and itself, and we denote it as Z_{eg}.

In the common mode equivalent circuit of Fig. 4, without considering the filter effects, the differential output voltage V_{ab} for an ideal opamp can be written as

$$V_{ab} = \frac{j\omega C_s R_2 Z_{eg}(Z_{ea} - Z_{eb})}{(Z_{ea} + Z_{eb} + 2R_1)Z_{eg} + (Z_{ea} + R_1)(Z_{eb} + R_1 + R_2) + j\omega C_s (Z_{ea} + R_1)(Z_{eb} + R_1 + R_2)Z_{eg}} V_c \quad (1)$$

where C_s is a stray capacitance between the ECG circuit ground and the earth ground. It should be noted that in the equivalent circuit of Fig. 4, only the stray capacitance C_s between the human body and the earth ground is dependent on the human body

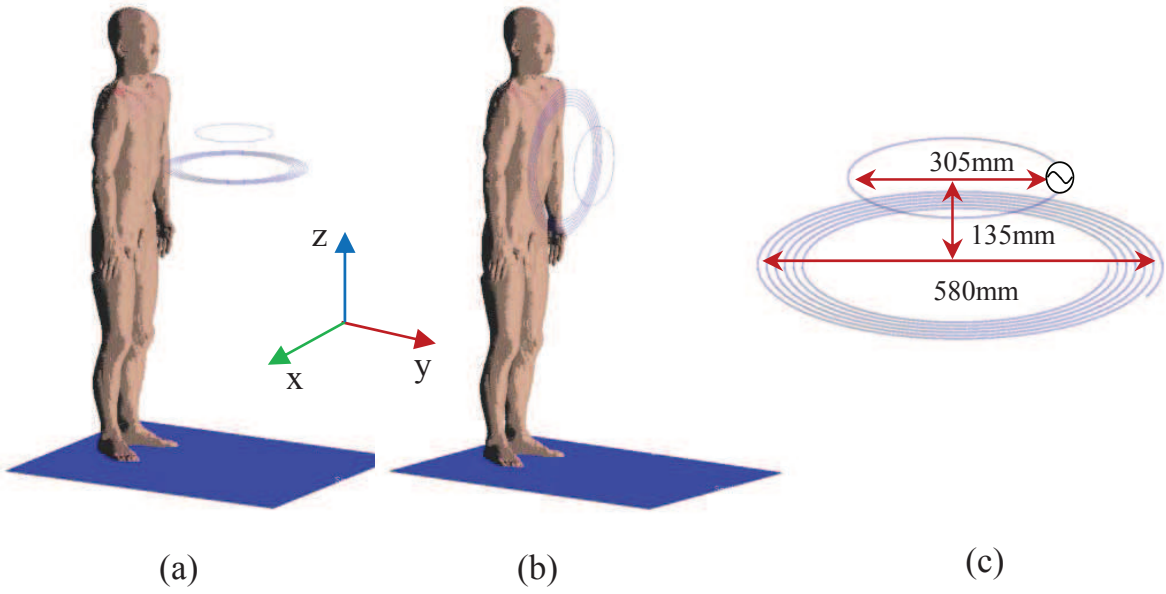

Figure 2. Numerical model of the wireless power transfer system at 6.8 MHz near a human body with a wearable ECG. (a)Horizontal arrangement of the drive loop and transmit coil, (b)vertical arrangement of the drive loop and transmit coil, (c)structure of the drive loop and transmit coil.

size or posture. When the human body is larger, the stay capacitance will increase due to the larger body's surface area. While when the human body is seated, the stray capacitance will also increase because larger body surface areas close to the earth ground. A calculation method for the stray capacitance can be found in [14]. With the common mode voltage V_c as the input to the equivalent circuit, we can calculate the differential mode voltage V_{ab} using Eq. (1). For an non-ideal opamp, we can use a circuit simulation tool such as SPICE (Simulation Program with Integrated Circuit Emphasis) to obtain the differential mode voltage V_{ab}. It can be seen from Eq. (1) that the differential mode voltage V_{ab} is converted from the common mode voltage V_c due to the imbalance between the two contact impedances Z_{ea} and Z_{eb}. If the two contact impedances are balanced, i.e., $Z_{ea} = Z_{eb}$, the common mode voltage V_c can not be converted into the differential mode voltage V_{ab}. In addition, if the ground electrode is well contacted with the human body so that the impedance Z_{eg} between the ground electrode and the human body is zero, the voltage V_{ab} can also be zero, although this is difficult to realize.

Then we employed a two-step approach to make the EMI evaluation for the wearable ECG. In the first step, we calculated the common mode voltages between the ECG electrodes and the earth ground using electromagnetic field simulation for an anatomical human body model, while in the second step, we evaluated the interference voltage at the ECG output using circuit

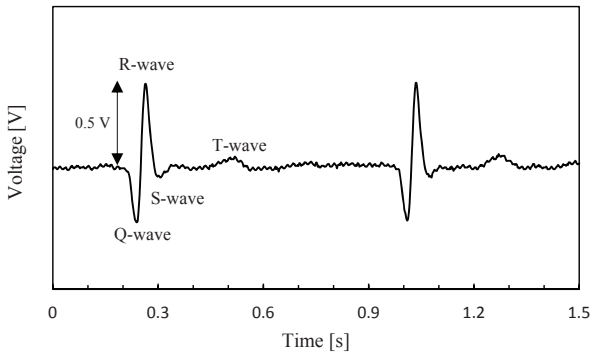

Figure 3. Example of ECG time waveform acquired by a HBC-based wearable ECG.

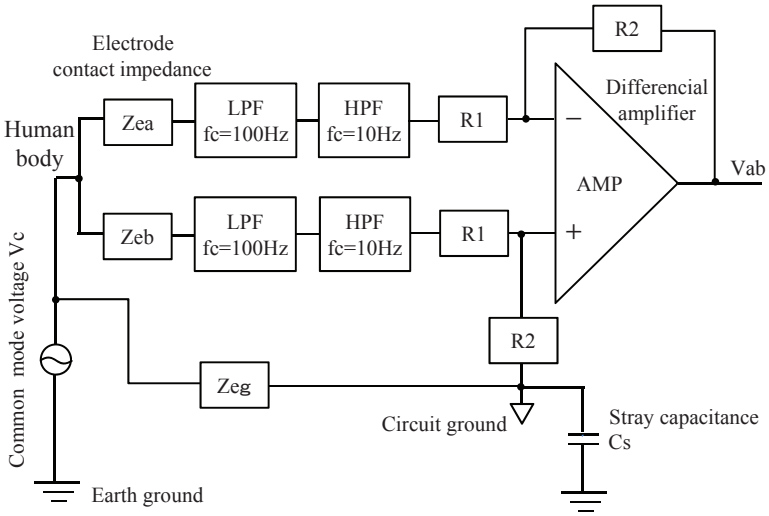

Figure 4. Common mode equivalent circuit of the wearable ECG.

simulation or measurement.

Electromagnetic Field Analysis Results

In the first step, we calculated the common mode voltage for the two arrangements shown in Fig. 2. We employed the full-wave finite difference time domain (FDTD) method together with an anatomical human body model. The FDTD method solves Maxwell's equation in time domain. By discretizing the analysis space into a number of small voxels and assigning each voxel to the corresponding permittivity and conductivity, this method adapts very well to model a human body. The human body model was developed based on the magnetic resonant image data of a Japanese adult [11]. It has a height of 173 cm, a weight of 65 kg, and consists of 51 types of tissue with a voxel size of 2 mm. The permittivity and conductivity of each tissue were cited from [12]. It is worth noting that the internal tissue structure is actually unimportant because the human body can be considered almost as a conductor at the investigated frequency.

The drive loop and transmit coil were arranged in a horizontal plane and vertical plane, respectively, in front of the human body. They were made of copper, and modeled as perfect conductor in the simulation. The drive loop was fed with a voltage source with an inner resistance of 50 Ω and a series capacitance of 450 pF for matching. The parameters of full-wave FDTD simulation were as follows. The analysis space enclosing the human body and the wireless power transfer system was 1.24 m × 1.04 m × 2.03 m. The voxel size δ ranged from 2 mm to 4 cm, which means that we employed a multi-grid FDTD algorithm where the detailed structure was modeled with 2 mm cells and the other parts were modeled with larger cells up to 4 cm at maximum. Such a multi-grid algorithm provides the almost same accuracy as modeling the entire analysis space with 2 mm cells. Even changing the minimum cell sizes from 2 mm to 10 mm, the difference on the calculated common mode voltage was within 5% at 6.8 MHz. Moreover, the time step was set to satisfy $\delta/\sqrt{3}c$, where c is the speed of light, to ensure numerical stability. The time stepping was performed for about 20 sinusoidal cycles to reach a steady state. To absorb outgoing scattered waves, the perfectly matched layer absorbing boundary conditions were used.

To confirm the FDTD modeling of the wireless power transfer system, we first conducted a simulation at 8 MHz as described in [10] in the absence of the human body. The result showed the same electric field distributions in front of the system for a transmit coil current of 1 A_{RMS} at resonance. We then added the human body model to the simulation, and derived the common mode voltages in both the horizontal arrangement and vertical arrangement of the transmitter system at 6.8 MHz. The common mode voltage $\dot{V}_c$ is a phasor quantity, and is related to the FDTD-calculated complex electric field $\dot{E}$ by $\dot{V}_c = \int_l \dot{E} \cdot dl$. It is thus available to calculate the complex common mode voltage $\dot{V}_c$ by integrating the complex electric field $\dot{E}$ along a route l from the ground plane to the chest surface (the attachment position of wearable ECG). The magnitude V_c of the complex common mode voltage $\dot{V}_c$ was then obtained by taking its absolute value.

Fig. 5 shows the FDTD-simulated electric field distribution at 6.8 MHz. The electric fields were found to distribute mainly outside the human body, and are quite weak inside the human body. Moreover, the vertical arrangement yielded a wider area of electric field distribution along the human body, so that the produced common mode voltage was larger. Although the attachment locations of electrodes were different on the chest, the obtained common mode voltages at different attachment

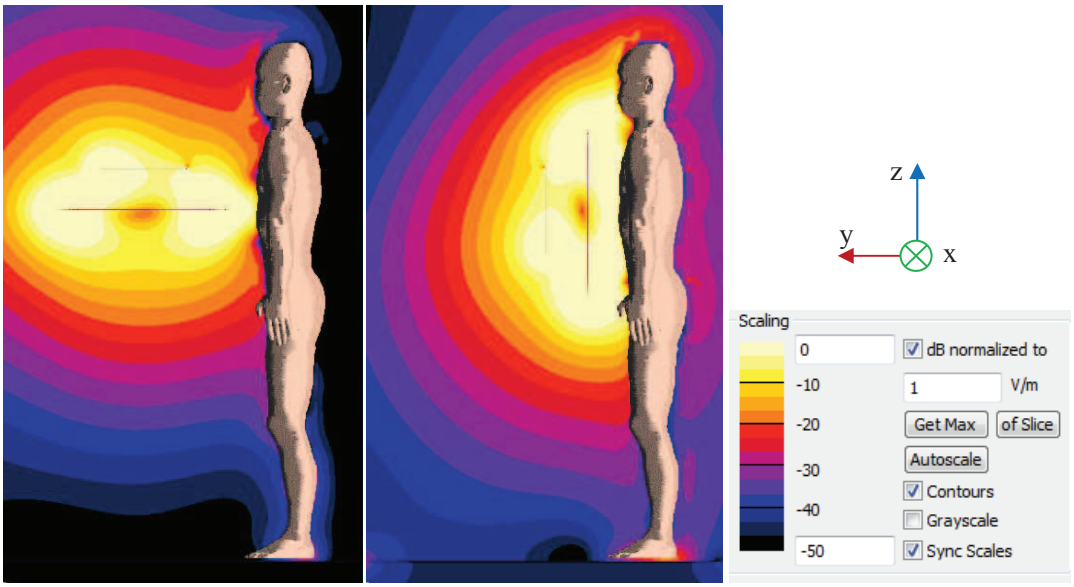

(a) (b)

Figure 5. Electric field distributions around the human body at 6.8 MHz. (a)Horizontal arrangement of the drive loop and transmit coil, (b)vertical arrangement of the drive loop and transmit coil.

Table 1. Common model voltage V_c produced by the 6.8 MHz wireless power transfer system

Arrangement	d = 1 cm	d = 10 cm
Horizontal	0.50 V	0.39 V
Vertical	1.36 V	1.24 V

Transmit coil current = 1 A_{rms}

locations were in a difference smaller than 10%. So it is reasonable to assume the same common mode voltage V_c between any electrode location on the human body and the ground plane. Table 1 shows the calculated common mode voltages for 1 A_{RMS} transmit coil current in the 6.8 MHz wireless power transfer system. The common mode voltage was larger at the vertical arrangement than that at the horizontal arrangement. This result exhibits the same trend observed from the electric field distributions in Fig. 5. Moreover, the common mode voltage decreased about 10% - 30 % when the distance between the transmit coil and the human body changed from 1 cm to 10 cm.

Circuit Analysis Results

As can be seen from Eq. (1), the differential mode voltage at the ECG output depends on the imbalance between the two sensing electrodes of the wearable ECG. The produced differential mode voltage is added to the actual ECG signal and interfere with it. To quantify the interference voltage level, we then conducted circuit simulation with SPICE for different impedance imbalances under both direct contact (resistive impedance) and non-direct contact (capacitive impedance) conditions of the electrodes.

Table 2 summarizes the parameters used in the circuit simulation. Without losing generality, the LPF and HPF were assumed to have an outside-band attenuation of 30 dB, and the differential amplifier has a gain of 60 dB for achieving nearly 1 V for AD converter. This means that the outside-band noise such as the wireless power transfer signal was approximately increased 30 dB. We therefore set $R_2 = 31.6\,R_1$ in Fig. 4 and Eq. (1) for considering the filters' influence. In addition, when the sensing electrodes are touched directly to the human body, the contact resistances R_{ea} and R_{eb} were assumed between 10 kΩ and 100 kΩ based on the literature [13]. When the sensing electrodes were not touched directly to the human body, the coupling capacitances C_{ea} and C_{eb} were assumed between 30 pF and 300 pF based on the square plate's size and spatial interval from the body surface. In addition, for convenience, we assumed the ground impedance Z_{eg} equal to Z_e or $1/j\omega C_e$, respectively. As for C_s, the stray capacitance between the circuit ground and the ground plane, in view of that the circuit was attached to the human body, we assumed it having a similar value to the human body capacitance of 200 pF.

Table 2. Circuit parameters for simulation

Direct contact: Resistive impedance	$Z_{ea} = R_{ea}$, $Z_{eb} = R_{eb}$
R_e: the average of R_{ea} and R_{eb}	10 kΩ - 100 kΩ
R_{ea} and R_{eb}	R_e ±10%, ±30%, ±50%
Non-direct contact: Capacitive impedance	$Z_{ea} = 1/j\omega C_{ea}$, $Z_{eb} = 1/j\omega C_{eb}$
C_e: the average of C_{ea} and C_{eb}	30 pF - 300 pF
C_{ea} and C_{eb}	C_e ±10%, ±30%, ±50%
R_1	10 kΩ
R_2	316 kΩ
Z_{eg}	R_e or $1/j\omega C_e$
Stray capacitance C_s	200 pF

Table 3. Differential mode interference voltage V_{ab} [mV] under direct contact condition for 1 A_{rms} transmit coil current

	d = 1 cm		d = 10 cm	
Imbalance	Horizontal	Vertical	Horizontal	Vertical
10%	63.3	172.2	49.4	157.0
30%	171.0	465.1	133.4	424.1
50%	262.7	714.4	204.9	651.4

The average R_e of R_{ea} and R_{eb} = 100 kΩ, and R_{eg} = 100 kΩ

Then at 6.8 MHz, with the common mode voltage V_c listed in Table 1 as the input, we calculated the differential mode voltage V_{ab} for different imbalances between R_{ea} and R_{eb} or C_{ea} and C_{eb} using both Eq. (1) and SPICE simulation. Tables 3 and 4 summarize the calculated results for 1 A_{rms} transmit coil current under different conditions. It should be noted that the calculated differential mode voltage V_{ab} values completely agree with the SPICE-simulated ones when the opamp is ideal, which ensures the validity and usefulness of both Eq. (1) and SPICE simulation in quantifying the EMI interference voltage.

From Tables 3 and 4 it can be found that, for the 6.8 MHz wireless power transfer system, the produced differential mode voltage is larger under the direct contact condition than the non-contact condition. Under the non-contact condition, the contact impedance between the sensing electrodes and the human body was capacitive, and its magnitude at 6.8 MHz was much smaller than the resistive impedance under the contact condition. The small impedance made the common mode voltage be difficult to be coupled into the ECG detection circuit. It was also found that that the vertical arrangement of the transmit coil resulted in larger interference voltage. This can be understood from the electric field distribution in Fig. 5 which suggests a larger common mode voltage in the vertical arrangement of transmit coil. Moreover, with the increase of the distance between the transmit coil and the human body, the produced differential mode voltage decreases significantly. For 1 A_{rms} transmit coil current, even at a distance of 10 cm, the differential mode interference voltage may achieve more than 0.6 V under the direct contact condition and 0.1 V under the non-contact condition for an impedance imbalance of 50%. The 0.6 V interference voltage may completely mask the entire ECG signal, and the 0.1 V interference voltage may make the acquisition of P-, Q- and T-waves difficult. So the influence on wearable ECG of a wireless power transfer system can not be ignored, and should be evaluated in the design stage. The two-step approach proposed in this study provides a useful means for this purpose.

Moreover, the contact impedance between the ground electrode and human body was found to play an important role in reducing the interference voltage. Figs. 6 and 7 show the dependence of R_{eg} and C_{eg} on the differential mode voltage V_{ab}, respectively. As can be seen, making the contact impedance as small as possible, i.e., the contact resistance as small as possible or the coupling capacitance as large as possible, can significantly reduce the interference voltage converted from the common

Table 4. Differential mode interference voltage V_{ab} [mV] under non-direct contact condition for 1 A_{rms} transmit coil current

	d = 1 cm		d = 10 cm	
Imbalance	Horizontal	Vertical	Horizontal	Vertical
10%	6.7	18.1	5.2	16.5
30%	21.7	58.9	16.9	53.7
50%	43.8	119.1	34.2	108.6

The average C_e of C_{ea} and C_{eb} = 30 pF, and C_{eg} = 30 pF

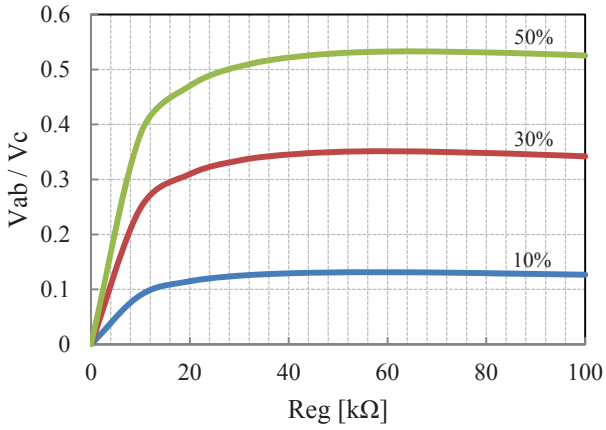

Figure 6. Dependence of R_{eg} between the ground electrode and the human body on the differential mode voltage V_{ab}. The average R_e of R_{ea} and R_{eb} is set equal to R_{eg} = 100 kΩ.

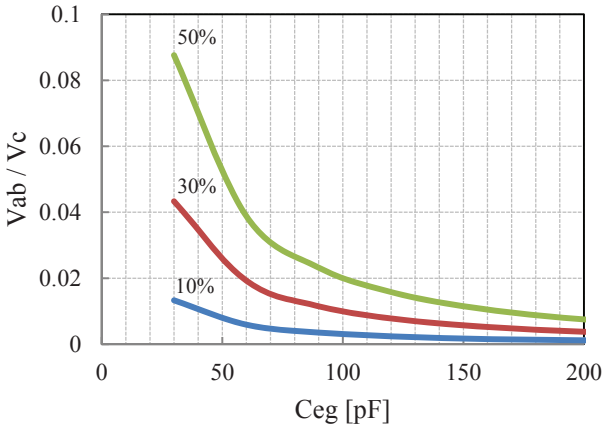

Figure 7. Dependence of C_{eg} between the ground electrode and the human body on the differential mode voltage V_{ab}. The average C_e of C_{ea} and C_{eb} is set equal to C_{eg} = 30 pF.

mode noise. This finding is also very useful in design a wearable ECG with high immunity to interference from a wireless power transfer system.

Experimental Verification

To verify the validity of the calculated interference voltage, we fabricated the common mode equivalent circuit and experimentally measured the differential mode voltage V_{ab} when changing the imbalance of the contact resistances R_{ea} and R_{eb} of sensing electrodes. The equivalent circuit modeled a direct contact condition of ECG electrodes, and a common mode voltage V_c produced by the 6.8 MHz wireless power transfer system was used as the input to the equivalent circuit. The average R_e of R_{ea} and R_{eb} of contact resistance was changed from 10 - 100 kΩ, and the imbalance between R_{ea} and R_{eb} was set to 10%, 30% and 50%, respectively. Fig. 8 shows the SPICE-simulated and measured V_{ab} with respect to V_c, denoted by lines and symbols respectively. It can be seen that the simulated interference voltages agree with the measured ones in a reasonable accuracy, which supports the validity of the employed approach and simulated results. In addition, it is also evident that the common-mode-produced interference voltage V_{ab} is not so sensitive to the contact resistance itself. It is mainly contributed from the imbalance of contact impedance of electrodes. So, making the impedance imbalance as small as possible is the most effective means to reduce the common-mode-produced interference voltage for a wearable ECG.

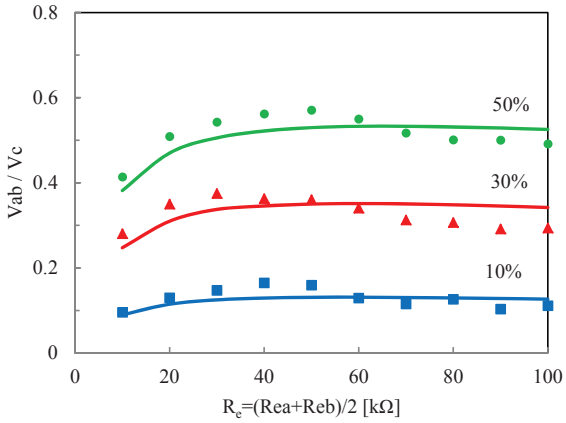

Figure 8. Comparison of SPICE-simulated and measured interference voltage V_{ab} produced by the imbalance between the contact resistance R_{ea} and R_{eb} for common mode input voltage at 6.8 MHz. Lines: SPICE-simulated, symbols: measured.

Conclusion

Electromagnetic compatibility consideration is essential in designing a wireless wearable device such as wearable ECG, and the wireless power transfer system may be a potential candidate to interfere with it. To evaluate the interference voltage against a wireless power transfer system, we have clarified that the interference voltage appearing at the ECG detection circuit is due to a conversion of common mode to differential mode voltages. We have employed a two-step approach, which combines an electromagnetic field analysis and an electric circuit analysis, to quantify the interference voltage for a 6.8 MHz wireless power transfer system. In the electromagnetic field analysis, the FDTD method was used to derive the common mode voltage between the human body and a ground plane. While in the electric circuit analysis, the SPICE has been used to calculate the common-mode-produced differential mode interference voltage at the output of ECG detection circuit. This two-step approach first time provides an effective means to quantitatively evaluate the EMI of wireless power transfer system for wearable healthcare devices in the design stage. As a result of the EMI evaluation, we have found that, for 1 A_{rms} transmit coil current, even at a distance of 10 cm from the human body, the interference voltage V_{ab} may achieve more than 0.6 V under the direct contact condition and 0.1 V under the non-contact condition for an impedance imbalance of 50%. The 0.6 V interference voltage may completely mask the entire ECG signal, and the 0.1 V interference voltage may make the acquisition of P-, Q- and T-waves difficult. The actual EMI voltage level depends on the filters' outside-band attenuation and the gain of the differential amplifier in the ECG detection circuit. To suppress such an interference, it has been found that making the imbalance between the two contact impedances of electrodes as small as possible is absolutely essential. It also should be noted that a larger outside-band attenuation of the LPF and HPF is also effective to suppress the interference level.

In conclusion, the presented approach is certainly useful in design stage of electromagnetic compatibility of wireless power transfer system, and is also available to be applied to any wearable device.

References

1. Wang, J., Wang, Q.: 'Body Area Communications' (Wiley-IEEE, 2012)
2. Astrin, A.W., Li, H.-B., Kohno, R.: 'Standardization for body area networks', IEICE Trans. Commun., 2009, E92-B, (2), pp.366–372
3. Monton, E., Hernandez, J.F., Blasco, J.M., et al.: 'Body area network for wireless patient monitoring', IET Commun., 2008, 2, (2), pp.215-222
4. Nemati, E., Deen, M.J., Mondal, T.: 'A wireless wearable ECG sensor for long-term applications', IEEE Commun. Mag., 2012, 50, (1), pp.36-43
5. Wang, J. Fujiwara, T., Kato, T., Anzai, D.: 'Wearable ECG based on impulse radio type human body communication', IEEE Trans. Biomed. Eng., 2015, DOI 10.1109/TBME.2015.2504998
6. Musavi, F., Eberle, W.: 'Overview of wireless power transfer technologies for electric vehicle battery charging', IET Power Electron., 2013, 7, (1), pp.60-66

7. Xie, L., Shi, Y., Hou, T., Lou, W.: 'Wireless power transfer and applications to sensor networks', IEEE Wireless Commun., 2013, 20, (4), pp. 140-145
8. Liao, W., Shi, J., Wang, J.: 'An approach to evaluate electromagnetic interference with wearable ECG at frequencies below 1 MHz', IEICE Trans. Commun., 2015, E98-B, (8), pp.1606-1613
9. Sample, A., Meyer, D., Smith, J.: 'Analysis, experimental results, and range adaptation of magnetically coupled resonators for wireless power transfer', IEEE Trans. Ind. Electron., 2010, 58, (2), pp. 544–554
10. Christ, A., Douglas, M.G., Roman, J.M., et al.: 'Evaluation of wireless resonant power transfer systems with human electromagnetic exposure limits', IEEE Trans. Electromagn. Compat., 2013, 55, (2), pp.265-274
11. Nagaoka, T., Watanabe, S., Saurai, K., et al.: 'Development of realistic high-resolution whole-body voxel models of Japanese adult males and females of average height and weight, and application of models to radio-frequency electromagnetic-field dosimetry', Phys. Med. Biol. 2004, 49, (1), pp.1-15
12. Available online: http://niremf.ifac.cnr.it/tissprop/
13. Spinelli, E.M., Martinez, N.H, Mayosky, M.A.: 'A transconductance driven-right-leg circuit', IEEE Trans. Biomed. Eng., 1999, 46, (12), pp.1466-1470
14. Fujiwara, O., Ikawa, T,: 'Numerical calculation of human-body capacitance by surface charge method', Trans. IEICE, 2001, J84-B, (10), pp.1841-1847

Acknowledgement

This work was supported in part by JSPS Grant-in-Aid for Scientific Research (Grant No. 15H04006).